

Alu repeated DNAs are differentially methylated in primate germ cells

Carol M. Rubin*, Catherine A. VandeVoort¹, Raymond L. Teplitz² and Carl W. Schmid³

Section of Molecular and Cell Biology, ¹California Regional Primate Research Center, ²Department of Medical Pathology and ³Section of Molecular and Cell Biology and Department of Chemistry, University of California at Davis, Davis, CA 95616, USA

Received April 21, 1994; Revised and Accepted October 19, 1994

ABSTRACT

A significant fraction of *Alu* repeats in human sperm DNA, previously found to be unmethylated, is nearly completely methylated in DNA from many somatic tissues. A similar fraction of unmethylated *Alus* is observed here in sperm DNA from rhesus monkey. However, *Alus* are almost completely methylated at the restriction sites tested in monkey follicular oocyte DNA. The *Alu* methylation patterns in mature male and female monkey germ cells are consistent with *Alu* methylation in human germ cell tumors. *Alu* sequences are hypomethylated in seminoma DNAs and more methylated in a human ovarian dysgerminoma. These results contrast with methylation patterns reported for germ cell single-copy, CpG island, satellite, and L1 sequences. The function of *Alu* repeats is not known, but differential methylation of *Alu* repeats in the male and female germ lines suggests that they may serve as markers for genomic imprinting or in maintaining differences in male and female meiosis.

INTRODUCTION

In vertebrate DNA, CpG dinucleotides are sites for methylation, forming 5-methylcytosine (5-meC). The frequency of CpG dinucleotides is lower than predicted by chance because 5-meC deaminates relatively rapidly to T (1). Cytosine methylation is essential to developing mammals, as mouse embryos having inactivated methyltransferase genes are non-viable (2). Differences in the amount of 5-meC found in male and female germline cells and the differential methylation of imprinted genes indicate that 5-meC may be involved in DNA imprinting; i.e., the mechanism by which male and female genomes are distinguished in a developing organism (3–5).

Alus are short (ca. 300 nt) interspersed million-fold repetitive sequences found in primates (6,7). Human *Alu* repeats belong to subfamilies of different evolutionary age (8,9). Young subfamilies (designated 'PV' and 'precise' herein) are nine-fold enriched in CpGs over total human DNA (9% vs. 1%). In older *Alu* subfamilies, many of these CpGs have decayed into TpG

or CpA, providing strong, albeit indirect, evidence for their germ line methylation (1,10). *Alu* repeats in spleen and brain DNAs are nearly completely methylated (11–13). This finding is significant, as *Alu* CpGs account for about one-third of the potential methylation sites in human DNA (13).

The pattern of *Alu* methylation in human sperm DNA is remarkably different from that in somatic tissue DNA (12,13). A subgroup of *Alu* repeats is unmethylated at a consensus *Bst*UI restriction site in human sperm DNA. *Alus* unmethylated at the *Bst*UI site are unmethylated at other sites and the PV family of young *Alus* is enriched in this subgroup. DNAs from seminoma and testis contain a similar subgroup of unmethylated *Alus* (13). Seminomas are derived from primary spermatocytes, and testis is enriched in mature and nearly mature male germ cells. Ovarian dysgerminomas are primary germ cell tumors classically referred to as 'seminomas of the ovary' (14, cited in 15), providing a female comparison to the methylation state of *Alus* in seminomas.

In this report, we show that the methylation level of *Alu* repeats in primate oocytes and dysgerminomas differs from that of sperm and seminomas. While primate sperm DNA is available in quantities sufficient to analyze by Southern blotting, a more sensitive assay is required to analyze the methylation of very small amounts of DNA available from primate oocytes. We describe the use of a sensitive linear PCR-based assay to determine the methylation pattern of *Alu* repeats in monkey oocytes and to compare this pattern with that found in human dysgerminoma tissue and in monkey sperm.

There are several possible interpretations of the differential methylation of *Alus* in germ cells. Methylation of *Alu* repeats may be associated with genomic imprinting in the two germ cells, either as a marker or a consequence. It is also possible that the contrasting levels of *Alu* methylation reflect differences in *Alu* transcriptional activity between the two germ cell types. RNA polymerase III transcription of *Alu* repeats is repressed by methylation *in vitro* (12,16).

Male and female germ cells also differ in their meiotic processes. Male germ cell meiosis is a continuous process, while female germ cells in mammals are suspended in the dictyotene (diakinesis I) stage of meiosis I from fetal development until

*To whom correspondence should be addressed

fertilization. It is possible that methylation of *Alu* sequences in oocytes is associated with the chromosomal structures characteristic of dictyotene. If *Alu* methylation plays a functional role in maintaining the oocyte's extended dictyotene state, the observed methylation pattern would have to be established before primary oocyte development.

MATERIALS AND METHODS

Human tumor tissues

Two ovarian dysgerminomas, 91-01-H02 and S93-406 were obtained from the Cooperative Human Tissue Network (CHTN), Pediatric Division. Pathology reports accompanying the dysgerminomas were confirmed by histological examination of each specimen (by RLT). The seminomas were obtained from the archives of the Department of Medical Pathology (UC Davis School of Medicine), and the diagnoses were confirmed by microscopic examination (by RLT).

Isolation and preparation of follicular oocytes

Ovaries were obtained from an adult rhesus macaque (*Macaca mulatta*) and were immediately placed in cold phosphate buffered saline (PBS) and refrigerated until processed. Ovaries were minced in PBS containing 0.4 mg/ml aprotinin (Sigma). All isolation and rinsing procedures were observed through a Nikon SMZ-2B dissection microscope. Oocytes were dissected from follicles with 25 gauge needles, transferred to a 35 mm petri dish containing 2 ml PBS and kept on ice. Each ovary yielded approximately 100 oocytes that were at least 75 μm in diameter. Oocytes were rinsed through a pulled Pasteur pipet to remove granulosa cells, placed in fresh PBS and refrigerated overnight. The next day, oocytes were rinsed twice by transfer to fresh PBS with a pulled Pasteur pipet. Oocytes prepared by this method appeared to be free of granulosa cells and debris when observed on an Olympus CK2 inverted stage microscope (Figure 1). Two separate oocyte preparations were analyzed.

Cytometric DNA quantitation in dysgerminoma tissue

For DNA quantitation, 7 μm paraffin sections of ovarian dysgerminoma were prepared. For hematoxylin and eosin staining

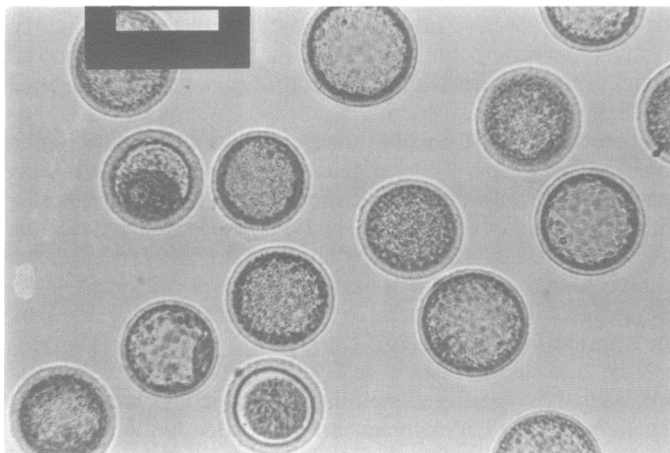


Figure 1. A typical oocyte preparation, demonstrating the absence of foreign cells and debris.

and light microscopic observation, 4 μm sections were prepared. Ploidy quantitation was performed on a Cell Analysis Systems (CAS) Model 200 image cytometer after Feulgen hydrolysis and staining with a CAS staining kit. Analyses were performed using a 280 μm filter with a 20 nm bandpass (18). A minimum of 25 nuclei from four separate quadrants of the tumor were measured to obtain a random sample and avoid measurement of a single clonally expanded population.

PV-selective and precise-selective blot hybridizations

The procedure outlined in (13) was used with the following modifications. DNA was transferred to Nytran+ charged nylon membranes (S&S) by the alkaline procedure recommended by the manufacturer. Membranes were UV crosslinked and oven dried, then hybridized for 16 h under non-stringent conditions (50°C, 5 \times Denhardt's/5 \times SSPE). All subsequent washes were performed in 5 \times SSPE, twice at room temperature for 5 min, and twice at higher temperatures (specified below) for 5 min.

Oligonucleotide 51 exactly matches the PV subfamily consensus sequence (Figure 2). When hybridized with oligonucleotide 51, the membrane was initially washed at the hybridization temperature to enhance signals. Subsequently, the filter was washed at higher temperatures (incremental to 60°C) to enrich for pairing with exact complements ('PV-selective' conditions). The change in membrane used and in the hybridization/washing conditions may result in less specific complementation of probe with immobilized DNA than previously reported (13). For these reasons, phosphorimager quantitations may not be comparable between these two studies. Oligonucleotide 71 exactly matches the precise *Alu* subfamily consensus sequence (Figure 2). The membrane was stripped and hybridized with oligonucleotide 71 at 50°C, then washed at a non-selective temperature (50°C).

DNA preparation for multicycle primer extension (MCPE)

DNA was isolated by standard methods (19) and digested for 2–3 h with *Rsa*I (Pharmacia), which does not cut the consensus *Alu* sequence. All digests were performed in New England Biolabs buffer #2. For end-labelling experiments, 1 μg of DNA was used. For dCTP incorporation experiments, 1–2 ng of DNA were digested. To lessen the chance of contamination of the minute amounts of DNA in the oocyte and control sperm preparations, these digestions were prepared with sterile water and fresh, unopened enzymes and buffers.

One-quarter of each digest was redigested with *Hpa*II, *Msp*I, *Bst*UI (New England Biolabs), or *Hha*I (Pharmacia) using 6–20 units overnight at the temperature recommended by the manufacturer. These conditions of considerable overdigestion were used to ensure complete cutting of susceptible sites in all samples.

MCPE assays using end-labelled primers

Five pmoles of oligonucleotide primer were end-labelled using reagents from the dsDNA Cycle Sequencing System kit supplied by GIBCO/BRL and γ -³²P dATP (5000 Ci/mmol, Amersham). The labeled primer was ethanol precipitated to remove unincorporated ATP, washed with 70% ethanol, dried, and resuspended in a small volume of water.

DNA digests were diluted in water to 10 ng/ μl . To ensure the same buffer conditions for all reactions, a master mix of PCR reagents (GeneAmp Core Reagents, Perkin Elmer Cetus), was

prepared according to the manufacturer's recommendations and 9 μ l aliquots were added to 1 μ l of DNA for a final reaction volume of 10 μ l. Forty-five cycles of 95°C for 1 min, 48°C for 1 min, and 72°C for 1 min were performed under mineral oil. Five μ l of formamide/dye mix were added to each reaction, the samples were heated for 2 min at 85°C, quick-chilled in ice water, and loaded onto an 8% denaturing polyacrylamide/urea gel. Gels were dried and quantitated on a Fuji BAS 2000 phosphorimager.

MCPE assays using dCTP incorporation

DNA from 50–60 oocytes was digested with each restriction enzyme in 10 μ l. Two μ l of each restriction digest (diluted to 25–50 pg/ μ l) was added to 10 μ l of reaction mix including 50 nM primer, 130 μ M dATP, 130 μ M dGTP, 130 μ M dCTP, 1.6 μ M dCTP, 0.825 μ M α^{32} -P dCTP (>6000 Ci/mmol, Amersham), 10 mM Tris–HCl pH 8.8, 2 mM MgCl₂, 50 mM KCl, and 0.2 units of *Taq* DNA polymerase. Cycling was performed as above, except that extension at 72°C was lengthened

to 1.5 min to compensate for the low concentration of dCTP present. One μ g of tRNA and sodium acetate to 10% were added. Fifty μ l of chloroform was added and the aqueous droplet was aspirated into a clean tube to remove mineral oil. The sample was ethanol precipitated and resuspended in 9 μ l of water. Four μ l of formamide/dye mix was added and electrophoresis was performed as described above.

RESULTS

Multicycle primer extension assay reveals methylation status at selected sites

A multicycle primer extension (MCPE) run-off assay was developed to test methylation of *Alu* repeat restriction sites in picogram to nanogram quantities of primate DNA. Three neighboring or overlapping restriction sites for the enzymes *Hpa*II/*Msp*I, *Hha*I, and *Bst*UI are clustered near the 5' end of the consensus *Alu* sequence (Figure 2). *Msp*I is not inhibited by

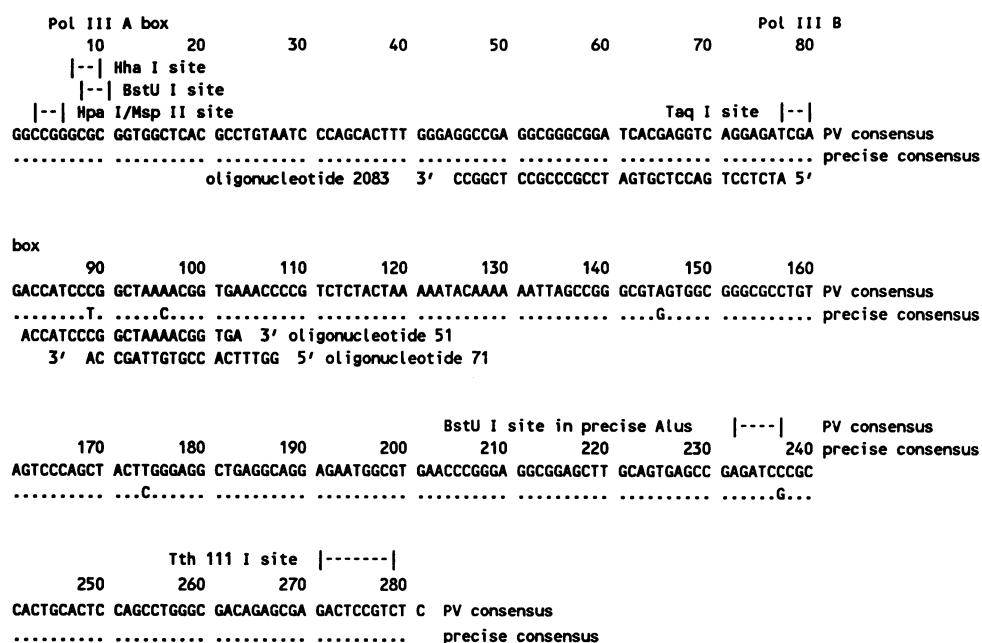


Figure 2. The consensus nucleotide sequence of the *Alu* PV and precise subfamilies showing the location of restriction sites and oligonucleotides referred to in the text.

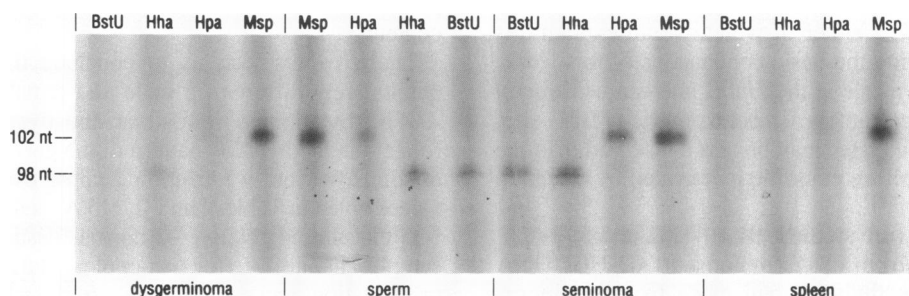


Figure 3. MCPE products for male and female germline tumors, human sperm, and human spleen. Ten ng of DNA digested with *Rsa*I and *Bst*UI, *Hha*I, *Hpa*II, or *Msp*I was amplified with end-labeled oligonucleotide 71 and subjected to electrophoresis under denaturing conditions. Results of phosphorimager scans are shown in Table I. Positions of predicted bands deduced from a sequence marker are indicated.

Table I. Results of MCPE assays

Tissue	Ratio of band intensities			Number of trials
	<i>Bst</i> UI <i>Msp</i> I	<i>Hha</i> I <i>Msp</i> I	<i>Hpa</i> II/ <i>Msp</i> I	
human spleen	0.010 ± 0.02	0.053 ± 0.04	0.074 ± 0.09	five
human sperm	0.28 ± 0.05	0.39 ± 0.2	0.29 ± 0.1	six
human seminoma	0.32 ± 0.35	0.45 ± 0.57	0.49 ± 0.52	two
human dysgerminoma 91-01-H02	0.047 ± 0.04	0.16 ± 0.05	0.060 ± 0.3	three
human dysgerminoma S93-406	0.43	0.32	0.68	one
rhesus oocyte	0.045 ± 0.05	0.013 ± 0.01	0.072 ± 0.05	four
rhesus sperm	0.33 ± 0.12	0.11 ± 0.06	0.42 ± 0.07	five

Phosphorimager comparisons of band intensities. Background corrections were made for each band by subtracting a background reading close to the band.

the presence of 5-mCpG in its recognition site, but the other three enzymes will not cut sequences which incorporate 5-mC (20). Genomic DNA was digested with these restriction enzymes, denatured, then annealed to and extended from the desired primer with *Taq* DNA polymerase during several cycles. When sufficient material was available, end-labeled primers were used to minimize background. For rhesus oocyte and the control sperm experiments, α -³²P-labeled dCTP was incorporated. The primer used, oligonucleotide 71, matches the precise *Alu* subfamily sequence exactly (Figure 2), but was annealed under permissive conditions (48°C) and undoubtedly primes many other *Alus* as well. MCPE with a second primer which exactly matches all known subfamilies (2083, Figure 2) gave results comparable to oligonucleotide 71 (data not shown).

MCPE using *Alu*-specific primers on DNAs digested by these four enzymes generates results generally consistent with findings based on blot hybridization (12, 13; Figures 3 and 6, Tables I and II). While the targeted *Msp*I site in spleen DNA is cleaved, there is no apparent cleavage of the isoschizomeric *Hpa*II site and the adjacent *Hha*I and *Bst*UI sites (Figure 3). Spleen DNA *Alus* are almost completely methylated (11).

In human sperm and seminoma DNAs the targeted *Hpa*II, *Hha*I, and *Bst*UI sites are each hypomethylated (Figure 3; 12,13). Though monkeys certainly lack the PV subfamily (21), the methylation pattern of monkey sperm DNA digested with *Bst*UI, *Hpa*II, and *Msp*I is similar to that of human sperm (Figures 3 and 4, Table I). When digested with *Hha*I, monkey sperm yields a band roughly 1/4 as intense as the corresponding human sperm band (Table I). Since the population of rhesus *Alu* subfamilies is different from humans, the monkey *Alu* probed by this assay may be either more mutated or more methylated in sperm at the *Hha*I site than human *Alus*, either of which would explain this difference without affecting the basic conclusions of this work. For all samples, only cleavage at the *Hpa*II site can be directly compared with cleavage at its isoschizomeric *Msp*I site. Consensus *Hha*I and *Bst*UI sites may be less conserved than the *Msp*I/*Hpa*II site and therefore could be inactivated by mutation as well as methylation.

Two dysgerminomas were studied, 91-01-H02 and S93-406. By MCPE, *Alu* repeats from dysgerminoma 91-01-H02 DNA are significantly more methylated than those from seminoma DNA (Figure 3). This disparity suggests a potential difference in *Alu* methylation patterns between the female and male germ lines. Dysgerminoma 91-01-H02 was primarily composed of triploid cells (41% of the total). Dysgerminoma S93-406 was

Table II. Results of Southern Hybridization Assays

Human Tissue	Ratio of band intensities		Selectivity
	<i>Bst</i> UI/Tth 111 I	<i>Taq</i> I/Tth 111 I	
sperm	0.77		PV
sperm	0.40		precise
seminoma	0.47		PV
seminoma	0.38		precise
spleen	0		PV
spleen	0		precise
dysgerminoma 91-01-H02	0.044		PV
dysgerminoma 91-01-H02	0.045		precise
dysgerminoma S93-406	0.25		PV

Phosphorimager comparisons of band intensities. Background corrections were made for each band by subtracting a background reading taken as close as possible to the band.

much less uniform in appearance (pleiomorphic) than dysgerminoma 91-01-H02, and the tumor also was heavily infiltrated with lymphocytes. DNA from this dysgerminoma was relatively unmethylated (data not shown; reported in Tables I and II), but because of the tissue heterogeneity we are unable to analyze the methylation pattern of this sample conclusively. Neither dysgerminoma showed the major tetraploid component expected if these tumors arose from oocytes arrested in dictyotene (the developmental stage of the rhesus oocytes used in this study). Even though dysgerminoma and seminoma resemble their progenitors (oocyte and spermatocyte, respectively) in *Alu* methylation, tumorigenesis could also affect the methylation pattern observed in these transformed tissues and their DNA content.

These results lead us to conclude that *Alu* methylation is qualitatively different in male and female germ cells, and that *Alu* methylation in seminoma and dysgerminoma appears to reflect the methylation pattern of the germ cells from which they arise. However, we caution against overinterpretation of the values given in Tables I and II. DNA methylation in tumor tissues is often altered relative to normal tissue. Minor variations in sample handling (for example, during pipeting, ethanol precipitation, and gel loading) can cause large fluctuations when manipulating these small amounts of template. To permit comparisons between different samples and different assay techniques, cleavage at targeted sites was analyzed by a phosphorimager and the quantitative results of this analysis are

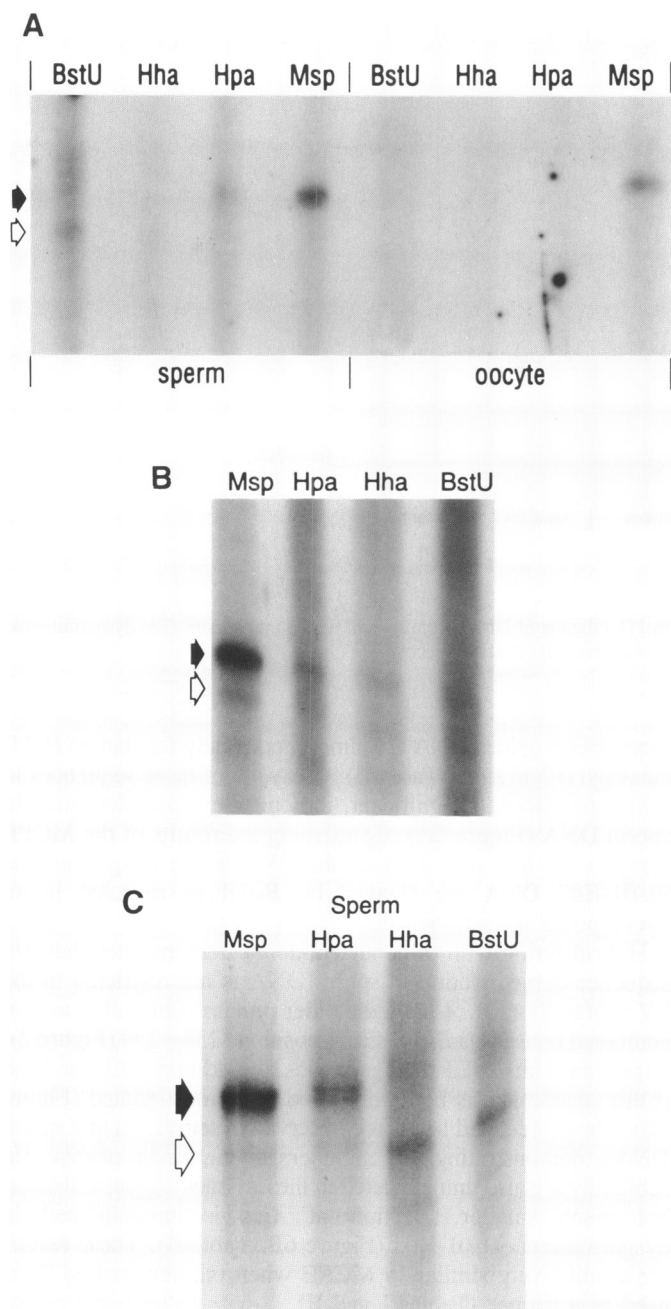


Figure 4. MCPE assays of two independent preparations of rhesus monkey oocytes. Approximately 50 pg of DNA was digested, amplified, and electrophoresed as indicated in Figure 4, except that α - 32 P CTP was incorporated into the products. The expected location of the *HpaII/MspI* band deduced from a sequencing marker is shown with a filled arrow; the *BstUI/HhaI* band location is shown with an outline arrow. Quantitations are given in Table I. (A) Sperm and oocyte preparations run simultaneously on the same gel. (B) A second oocyte preparation. (C) A second sperm control preparation.

reported in Tables I and II. The phosphorimager values displayed in Tables I and II are intended to provide a relative, rather than absolute, measure of the extent of *Alu* methylation in different tissues.

Follicular oocyte *Alus* are almost completely methylated

By incorporating multiple radionucleotides, the extremely sensitive MCPE method can assay *Alu* repeat methylation in the

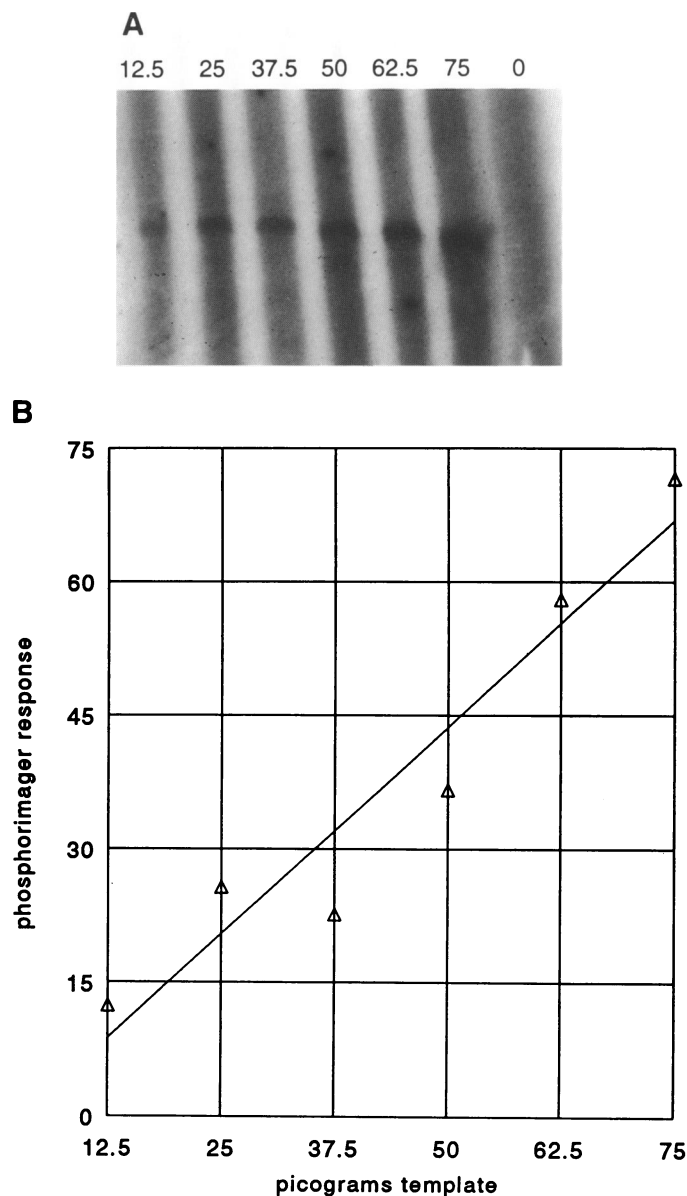


Figure 5. Different amounts of rhesus monkey sperm DNA digested with *MspI* were subjected to MCPE with incorporation of α - 32 P dCTP to demonstrate linearity of response with increasing template concentration. (A) Numbers above the lanes are picograms of template DNA loaded. (B) Least squares line plotted for data shown in A. The root mean square standard deviation is \pm 24%.

minute amount of DNA available from a limited number of primate oocytes. Linear response of this method was tested by measuring the amount of α - 32 P dCTP incorporated for different concentrations of *MspI*-digested monkey sperm DNA in a range approximating that of the oocyte DNA (Figure 5A). Qualitatively, incorporation increases as template concentration is increased from 12.5 to 75 pg (Figure 5A). The response is linear within \pm 24 % rms deviation, indicating the semiquantitative nature of the assay and its proportionality to cleavage at the tested sites (Figure 5B).

In agreement with this calibration, rhesus monkey sperm DNA yields equivalent results whether extended with labeled primer (results not shown) or with radionucleotide incorporation (Figure 4). The degree of methylation at the *BstUI* and *HpaII* sites in

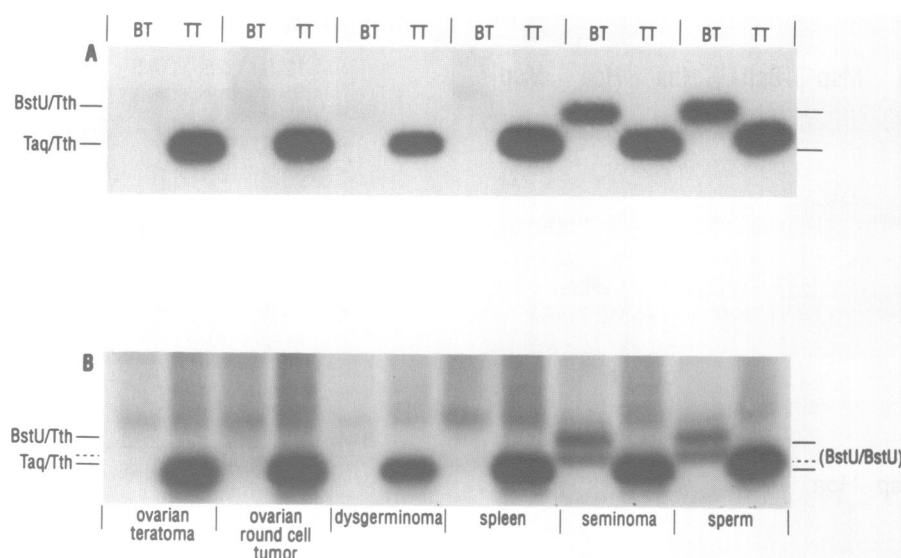


Figure 6. Human *Alu* subfamily selective hybridization of *Bst*UI/Tth 111 I and *Taq*I/Tth 111 I digests of DNAs from several tissues and tumors. The dysgerminoma shown is 91-01-H02. Phosphorimager quantitation is summarized in Table II. (A) PV-selective. (B) Precise-selective.

rhesus monkey sperm DNA *Alus* is also qualitatively similar to that of human DNA assayed by MCPE and by hybridization with oligonucleotide 71 (Tables I and II).

In marked contrast to monkey sperm preparations, the targeted *Hpa*II, *Hha*I, and *Bst*UI sites appear highly methylated in *Alu* repeats from rhesus monkey follicular oocytes (Figure 4A). A second preparation of monkey oocytes gave a similar result (Figure 4B). A faint background ladder in all lanes, attributable to premature truncations and cryptic *Rsa*I restriction sites in the diverged *Alu* template population, demonstrates both the presence of undegraded template *Alus* and active DNA polymerization, thereby providing an internal positive control (Figure 4A and B). Blank preparations with no template do not show this background ladder (Figure 5A). We conclude that *Alu* sequences detected by MCPE with oligonucleotide 71 are more methylated at the 5' end in monkey oocytes than in monkey sperm.

Blot hybridization confirms MCPE assay

Methylation of *Alu* *Bst*UI sites has been previously assayed by blot hybridization (11,13), and in this work we compare the results of the hybridization and MCPE assays. The appearance of a 265 nt band after digestion with *Bst*UI and Tth 111 I is diagnostic for an unmethylated, unmutated *Bst*UI site near the *Alu* 5' end (Figure 2). A *Taq*I site at position 77 (Figure 2) is indifferent to cytosine methylation (20). Double digestion of human DNA with *Taq*I and Tth 111 I (which cleaves at position 274, Figure 2) releases a 196 nt restriction fragment providing a measure of total *Alu* DNA present (11,13).

The results of this experiment depend critically on hybridization conditions. At 60°C, oligonucleotide 51 selectively hybridizes to PV *Alu* repeats (Figure 6A, Table II). Oligonucleotide 71 exactly matches precise *Alus*, but was hybridized and washed at a non-selective temperature, 50°C (Figure 6B, Table II). In older *Alu* repeats sequence divergence, as well as methylation, inactivates the consensus *Bst*UI site.

In agreement with previous results (13), the majority of PV *Alu* repeats in sperm DNA are cleaved by *Bst*UI whereas these

sequences in spleen DNA are almost completely resistant to *Bst*UI cleavage (Figure 6A, Table II). Cleavage of these sequences in seminoma DNA is significant, although less complete than in sperm DNA (Figure 6A). Confirming the results of the MCPE assay, very few (*ca.* 4%) of the PV *Alus* in dysgerminoma 91-01-H02 DNA are cleaved by *Bst*UI as revealed in an overexposed autoradiogram.

Hybridization with oligonucleotide 71 demonstrates that *Alu* sequence demethylation in sperm DNA is not restricted to the PV subfamily (13). *Alus* in the older precise subfamily have an additional consensus *Bst*UI site at positions 236–239 (Figure 2). Digestion with *Bst*UI thus generates an additional 225 nt band if this second site is both conserved and unmethylated (Figure 6B). These predicted bands are observed in seminoma and sperm DNAs, demonstrating that members of the larger precise *Alu* subfamily are also unmethylated in these tissues. Again a distinct, but much smaller, fraction of *Alus* is unmethylated in dysgerminoma 91-01-H02 (Figure 6B, Table II). These results are qualitatively similar to MCPE when oligonucleotide 71 is used as a primer (Tables I and II).

DISCUSSION

Alu sequences are hypomethylated in sperm DNA (12,13). Indeed, Hellmann-Blumberg *et al.* (13) find that demethylation at the *Bst*UI site in the *Alu* A box (Figure 2) is predictive of demethylation at other CpG-containing restriction sites in these *Alus*. While most young (PV) *Alus* are found in this fraction (the 'BstU' subset), *Alu* sequences from other subfamilies are also present. Sperm and spleen DNAs represent extremes in tissue-specific methylation of *Alu* repeats (12,13; Tables I and II).

As demonstrated by MCPE and hybridization, *Alus* in both monkey oocyte and human female germline tumor DNAs are almost fully methylated (Figures 3 and 6). The differential methylation of *Alus* in the male and female germ lines requires this pattern to be developmentally controlled.

Monk *et al.* (22) show that total mouse DNA is more methylated in sperm than in oocyte. Sanford *et al.* (23,24) determined that mouse satellite DNAs are undermethylated in both sperm and oocyte DNA compared with somatic tissue DNAs. Human α satellite DNA is also undermethylated in sperm relative to brain or placenta (25). L1 repeats (another abundant interspersed family) are at least five times less methylated in mouse oocyte DNA than in sperm DNA (24,26). Differences in germ cell methylation have also been determined for several loci within or near genes. With the exception of inactivated X chromosomes, CpG islands (i.e., DNA sequences locally rich in CpG sites) are unmethylated (27). Non-island CpG sites are completely methylated in sperm and are often methylated in oocyte DNA (28,29). Thus, hypermethylation in oocytes and hypomethylation in sperm is a pattern unique to *Alu* sequences.

Hypomethylation in sperm does not affect all *Alus*, or even all young *Alus* (Figure 6, Table II). Though Hellmann-Blumberg *et al.* (13) found that most PV *Alus* are completely demethylated in sperm, Kochanek *et al.* (12) show that a member of the youngest (PV) *Alu* subfamily is completely methylated in all tissues tested, including human sperm, while a member of the next youngest subfamily (precise) is completely demethylated in sperm. Obviously, while age of the *Alu* insert is important, other factors such as chromosomal location, position relative to CpG islands, and the nucleotide environment of the *Alu* may also help determine the extent of methylation.

DNA methylation is thought to encode genomic imprinting (4,5,30). Barlow (5) and Varmuza and Mann (4) have proposed that a gametic imprint marks the chromosomes from each parent and signals the establishment of the actual somatic imprint which causes functional differences between the chromosomes in the developing zygote. Ubiquitous, interspersed, differentially methylated CpG-rich *Alu* repeats could be the genome-wide difference required for gametic imprinting in this model.

DNA methylation also inhibits transcription of *Alu* templates (16,17), and differential methylation in sperm and oocyte may reflect a need to regulate production of *Alu* transcripts differently in male and female germ cells. Alternatively, transcriptional activity might affect the *Alu* DNA methylation pattern by protecting transcribed regions from methylation. As another indication that the difference in *Alu* methylation between these two cell types is significant, a protein found in primate sperm (but not in HeLa cells) binds selectively with *Alu* sequences and inhibits CpG methylation (Chesnokov and Schmid, unpublished).

The difference in *Alu* methylation between male and female germ cells might play a role in imprinting, transcript regulation, or, as discussed in the Introduction, in their different meiotic processes. Though the function of *Alu* repeats remains unknown, their tissue-specific and differentially inherited CpG methylation suggests that these sequences are, in fact, functional for the organism.

ACKNOWLEDGEMENTS

This work was supported by USPHS grant GM21346 and by the Agricultural Experiment Station at the University of California, Davis. Tissue samples were supplied by the Cooperative Human Tissue Network, funded by the National Cancer Institute, and by the UCDMC Department of Pathology. The authors thank Utha Hellmann-Blumberg for helpful discussions regarding imprinting. Dr B.H.Min graciously performed the image cytometry for quantitative DNA.

REFERENCES

- Bird, A. (1980) *Nucleic Acids Res.*, **8**, 1499–1504.
- Li, E., Bestor, T.H., and Jaenisch, R. (1992) *Cell*, **69**, 915–926.
- Surani, M.A. (1993) *Nature*, **366**, 302–303.
- Varmuza, S., and Mann, M. (1994) *Trends in Genet.*, **10**, 118–123.
- Barlow, D.P. (1994) *Trends in Genet.*, **10**, 194–199.
- Schmid, C.W., Deka, N., and Matera, A.G. (1989) In Adolph, K.W. (ed.), *Chromosomes: Eukaryotic, Prokaryotic, and Viral*. CRC Press, Boca Raton, Vol. 1, pp. 3–29.
- Weiner, A.M., Deininger, P.L., and Efstratiadis, A. (1986) In Richardson, C.C., Boyer, P.B., Dawid, I.B., and Meister, A. (eds.), *Annual Rev. Biochem.*, Annual Reviews, Inc., Palo Alto, Vol. 55, pp. 631–661.
- Schmid, C.W. and Marais, R. (1992) *Current Opinion in Genetics and Development*, **2**, 874–882.
- Deininger, P.L., Batzer, M.A., Hutchison III, C.A., and Edgell, M.H. (1992) *Trends in Genet.*, **8**, 307–311.
- Jurka, J. and Milosavljevic, A. (1991) *J. Mol. Evol.*, **32**, 105–121.
- Schmid, C.W. (1991) *Nucleic Acids Res.*, **19**, 5613–5617.
- Kochanek, S., Renz, D., and Doerfler, W. (1993) *EMBO J.*, **12**, 1141–1151.
- Hellmann-Blumberg, U., McCarthy Hintz, M.F., Gatewood, J.M., and Schmid, C.W. (1993) *Mol. Cell. Biol.*, **13**, 4523–4530.
- Masson, P. (1912) *Bull. Soc. Anat.*, Paris **87**, 402–407.
- Teilum, G. (1976) *Special Tumors of Ovary and Testis and Related Extragonadal Lesions*, 2nd ed., J.B. Lippincott Co., Philadelphia, p 180.
- Liu, W.-M. and Schmid, C.W. (1986) *Nucleic Acids Res.*, **21**, 1351–1359.
- Liu, W.-M., Marais, R.J., Rubin, C.M., and Schmid, C.W. (1994) *Nucleic Acids Res.*, **22**, 1087–1095.
- Teplitz, R.L., Butler, B.B., Tesluk, H., Min, B.H., Russell, L.A., Jensen, H.M., and Hill, L.R. (1990) *Analyt. and Quant. Cytol. and Histol.*, **12**, 98–102.
- Sambrook, J., Fritsch, E.F., and Maniatis, T. (1989) *Molecular Cloning: a Laboratory Manual*, 2nd ed. Cold Spring Harbor Laboratory Press, Cold Spring Harbor.
- Nelson, M., Raschke, E., and McClelland, M. (1993) *Nucleic Acids Res.*, **21**, 3139–3154.
- Leefflang, E.P., Liu, W.-M., Chesnokov, I.M., and Schmid, C.W. (1993) *J. Mol. Evol.*, **37**, 559–565.
- Monk, M., Boubelik, M., and Lehnert, S. (1987) *Development*, **99**, 371–382.
- Sanford, J.R., Clark, H.J., Chapman, V.M., and Rossant, J. (1987) *Genes & Devel.*, **1**, 1039–1046.
- Sanford, J., Forrester, L., and Chapman, V. (1984) *Nucleic Acids Res.*, **12**, 2823–2836.
- Gama-Sosa, M.A., Wang, Y.-H., Kuo, K.C., and Gehrke, C.W., and Ehrlich, M. (1983) *Nucleic Acids Res.*, **11**, 3087–3095.
- Howlett, S.K. and Reik, W. (1991) *Development*, **113**, 119–127.
- Bird, A.P., Taggart, M., Frommer, M., Miller, O.J., and McLeod, D. (1985) *Cell*, **40**, 91–99.
- Kafri, T., M. Airel, M. Brandeis, R. Shemer, L. Urven, J. McCarrey, H. Cedar, and Razin, A. (1992) *Genes & Dev.*, **6**, 705–714.
- Shemer, R., Kafri, T., O'Connell, A., Eisenberg, S., Breslow, J.L., and Razin, A. (1991) *Proc. Natl Acad. Sci. USA*, **88**, 11300–11304.
- Li, E., Beard, C., and Jaenisch, R. (1993) *Nature*, **366**, 362–365.